

Morphology–Mechanical Property Relations in Syndiotactic Polypropylene (sPP) Fibers

JOACHIM LOOS* and TILO SCHIMANSKI

*Eindhoven Polymer Laboratories
Dutch Polymer Institute
P. O. Box 513, 5600 MB Eindhoven, The Netherlands*

Mechanical properties of melt-spun syndiotactic polypropylene single filament fibers were studied in relation to their formation conditions. Depending on the processing parameters, fibers with rubber-elastic properties can be prepared. Dynamic mechanical studies show almost unchanged rubber-elastic properties after 1000 test cycles. A model of the fiber morphology is introduced to explain the rubber-elastic behavior: small micel-like crystals containing molecules in the planar all-trans conformation act as physical crosslinks in the amorphous matrix.

INTRODUCTION

The syndiotactic form of polypropylene has historically received considerably less attention than the highly successful isotactic form. Until 1998, syndiotactic polypropylene (sPP) was not a commercial product available on a regular basis. Fina Oil and Chemical Company in the United States, a subsidiary of Petrofine of Belgium, and Mitsui Toatsu in Japan have produced experimental quantities. In 1993, Fina made the first reported commercial test run of sPP using a liquid full-loop reactor.

Produced by metallocene catalysts, even highly syndiotactic polypropylene (90%–95% syndiotacticity) has relatively low crystallinity because the syndiotactic block lengths in its molecular structure are short. Because of its relatively low crystallinity and small crystal size, sPP has high clarity and low density, hardness, tensile strength and stiffness compared with isotactic polypropylene (iPP). The crystallization rate, crystallization temperature, and melting temperature are all affected by the microtacticity of the resin (1).

Although sPP has been targeted for specialty markets, it may also compete against iPP, low density polyethylene (LDPE), linear low density polyethylene, polyethylene copolymers (LLDPE) and polyvinyl chloride (PVC) because of its toughness, impact strength (especially below the glass transition temperature), transparency and low heat seal temperature. Potential application areas include adhesives such as hot melt and functional grafting type adhesives, elastomers, extrusion and injection molded products that must be

sterilized by radiation, transparent sheets, films requiring high clarity, toughness and low heat sealing temperature, and fibers.

It has been shown that this polymer exhibits polymorphism in the solid state. Following a standard nomenclature (2), four different crystalline phases have been found: the crystalline form I and form II, both characterized by chains in helical $(ttgg)_n$ conformation (2–8), the crystalline form III (9–12), with chains in trans-planar $(tttt)_n$ conformation and the fourth modification, with chains in a $(t_6g_2t_2g_2)_n$ conformation being an intermediate between the helical and the trans-planar conformation (13, 14). The crystal structure of sPP has been extensively studied, but only a few reports on the physical and mechanical properties of sPP have been published (15–19). The upsurge in interest in sPP stems in part from the possibility that alternate positioning of methyl groups may favor an extended chain conformation (form III) and thus lead to mechanical properties more likely to polyethylene than isotactic polypropylene (measured crystalline moduli: iPP \sim 40 GPa (20); sPP_{form I + II} \sim 8 GPa (21); sPP_{form III} \sim 66 GPa (21)). It is the purpose of this report to present certain physical characteristics such as the static and dynamic tensile behavior of melt-spun sPP single filament fibers. Based on additional wide angle X-ray scattering (WAXS) data a morphological model will be introduced to explain the mechanical behavior of these fibers.

EXPERIMENTAL

The sPP used in the experiments was kindly supplied by the Fina Oil and Chemical Company. The material has a syndiotacticity of about 90%, a melting temperature of approximately 136°C, and a melt flow

*To whom correspondence should be addressed.

index (MFI) of 4. The molecular weight (Mw)/MFI relationships of sPP are different than iPP, for a given MFI the Mw of sPP is always lower than iPP. A Mw of 160,000 g/mol has been assumed for the investigated resin (22).

Single filament fibers with circular cross section were prepared by a single stage melt-spinning process using a laboratory-scale spin-draw device (Wiedmann 1-212, Germany) equipped with a capillary with a diameter of 1.35 mm and a length of 8 mm. The original sPP pellets were melted at 160°C in a double wallet cylinder, subsequently pressed through the capillary with flow speeds of approximately 0.02 m/min and 0.1 m/min, cooled in the air to room temperature, and wound with speeds varying from 5 m/min to 30 m/min. The spinning draw-down is defined as the ratio between the fineness (in units of tex = weight in grams per km length) of an unwound as spun fiber and the fineness of the wound fiber. Neither additional cold-drawing nor annealing was performed.

Mechanical properties of the fibers were determined using a Zwick 1445 tensile tester equipped with a 5 N load cell and special fiber clamps for standard tensile experiments. A Frank 81565 tensile tester was used for cyclic load-release experiments. Both experiments were carried out at ambient temperature with fibers of initial gauge length of 100 mm and with a crosshead speed of 50 mm/min. The cyclic load-release experiments were performed using a force-controlled mode in a range of 25% to 80% of the maximum load at fracture determined in the tensile tests. Mechanical data presented in this article are the average of ten parallels. Wide-angle X-ray measurements (WAXS) were performed on as-spun fibers at room temperature using a Philips pinhole camera.

RESULTS AND DISCUSSION

The tensile properties of melt-spun sPP fibers are influenced by their physical structure, which is controlled by the fiber formation conditions. Depending on the spinning draw-down, fibers with a wide range of fineness 1 tex to 58 tex, or of diameter 38 μm to 290 μm can be prepared (Fig. 1a), respectively. Typical stress-strain curves for as-spun single filament fibers are shown in Fig. 1b. Fibers with draw-down less than 100 show a yield point and the stress drops after the yield. This behavior indicates the development of necks and large plastic deformation sections before the stress starts to rise again followed by fracture of the fibers. The onset point at which the stress starts to rise (strain hardening) steadily decreases with increasing draw-down. The plastic deformation region essentially disappears above a draw-down of approximately 100, and for draw-down above 250 the fibers show rubber-like stress-strain curves without any indication for plastic deformation.

Figures 1c and 1d show plots of tensile strength and elongation at break versus draw-down of as-spun fibers, respectively. The tensile strength improves with

increasing draw-down, the highest value is observed for fibers with highest draw-down. The values of the elongation at break drop with increasing draw-down and asymptote at large draw-downs. The relative high elongation at break value of the data point with highest draw-down should be explained by experimental variations.

Except for as-spun fibers with low draw-down, a post drawing could not be performed. Independent of temperature and drawing loads, only an elastic elongation with final fracture of the fibers could be obtained. According to the work of Sakata *et al.* (17), a possible explanation for the poor drawability of sPP may be the absence of α -relaxation, which is assigned to an increased flexibility of grain boundaries (inter crystalline) and sliding of lamellar crystals (intra crystalline) in the spherulites (23). In contrast iPP shows a strong α -relaxation at approximately 100°C. For post-drawing temperatures above this relaxation temperature, iPP fibers have good drawability. Additional dynamic tensile tests were performed, and again the data sets indicate a rubber-like behavior of sPP fibers with draw-down above 250. Figure 2 shows stress-strain curves of continuous load-unload cycles for a fiber with high spinning draw-down of 1150 and a diameter of 38 μm , respectively. The data describe cycles starting with 25% and using an upper load limit of 80% of the average fracture load. The load part of the first cycle represents the equivalent part of the static tensile curve. Unloading of the fiber results in an almost complete elastic recovery, defined as the ratio between the recovered strain and the total applied strain. Additional to the elastic recovery, the hysteresis behavior of the first cycle indicates a low energy loss, represented by the area enclosed by the load-unload curves.

After ten cycles the appearance of the load-unload curve is almost congruent with the first cycle. Neither the overall shape of the curve nor the position in the stress-strain plot in case of initial and final values has been changed. Performing further load-unload cycles the curves start shifting to higher elongation values, however maintaining the original shape. This shift is a strong indication for non-reversible plastic deformation, but on a very low level. After 100 cycles the initial and final strain values are shifted about approximately 7% and after additional 1000 cycles a shift of 15% can be determined. These data correspond with an elongation of approximately 7% and 15% of the released fibers after 100 and 1000 load-unload cycles, respectively.

For an explanation of this unusual mechanical behavior of fibers prepared from a thermoplastic homopolymer, a detailed discussion of the stress induced crystallization of sPP and the resulting morphology-mechanical property relation is needed. In order to investigate the orientation and phase behavior, WAXS pinhole film patterns on spun fibers are obtained. Figure 3 shows a X-ray pinhole diffraction pattern of a bundle of melt-spun sPP fibers with draw-down 1150.

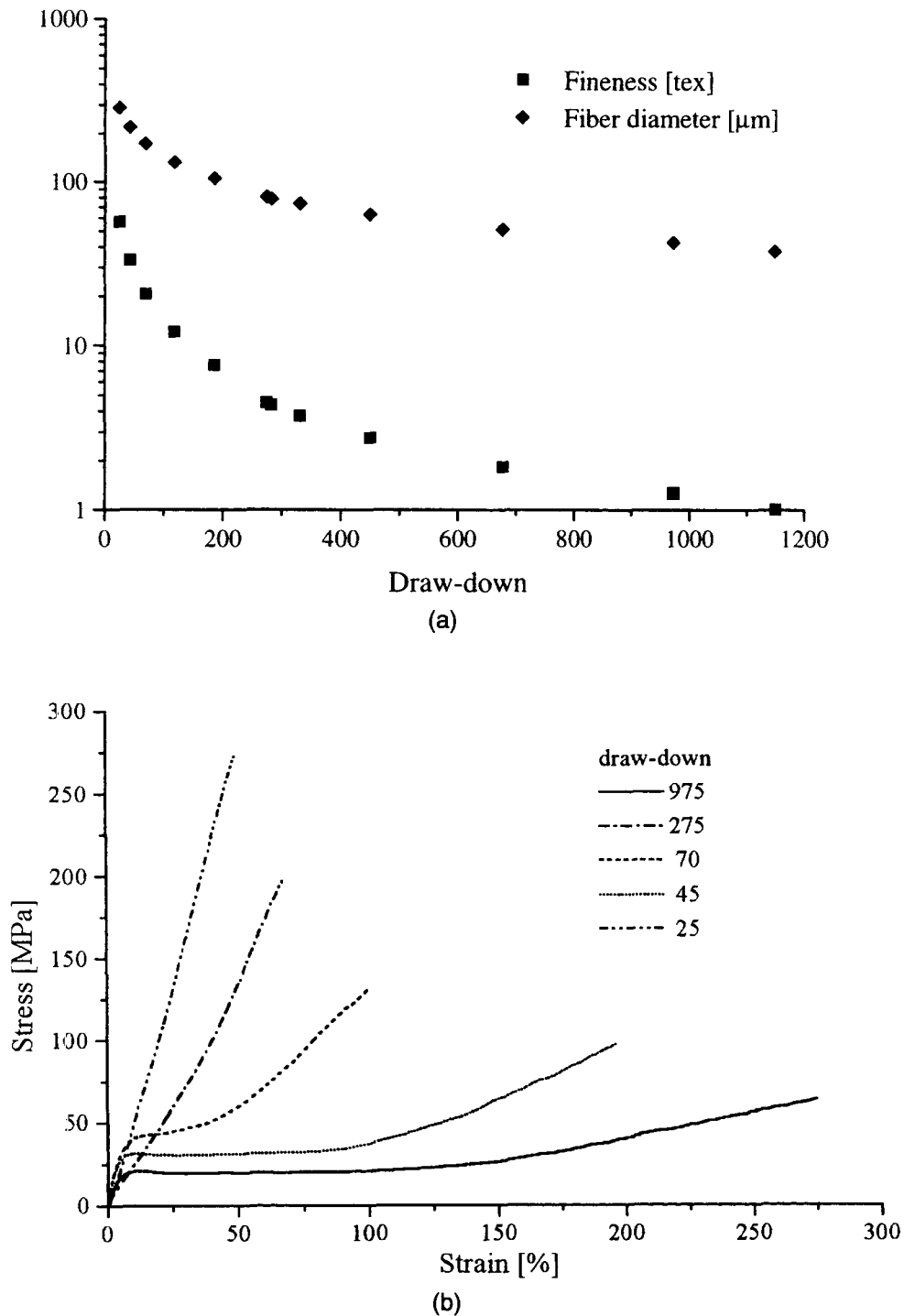


Fig. 1. Properties of melt-spun sPP fibers: a) log fineness/diameter vs. spinning draw-down, b) representative stress-strain plots for fibers with different spinning draw-downs; c) tensile strength vs. spinning draw-down; and d) elongation at break vs. spinning draw-down.

The main reflections are indicated. The diffraction pattern is explained in terms of an orthorhombic unit cell containing molecules with all-trans conformation (11). Additionally, the pattern shows a preferential orientation along the fiber axis, and the amorphous halo is fairly broad, indicating a low crystallinity of the

fibers. Using Scherrer's formula, the broadness of the (021), (020) and (110) reflections is assigned to small crystal sizes in the fibers.

Based on the data presented in this study a model connecting the observed mechanical behavior with the crystal phase formation and the morphology of

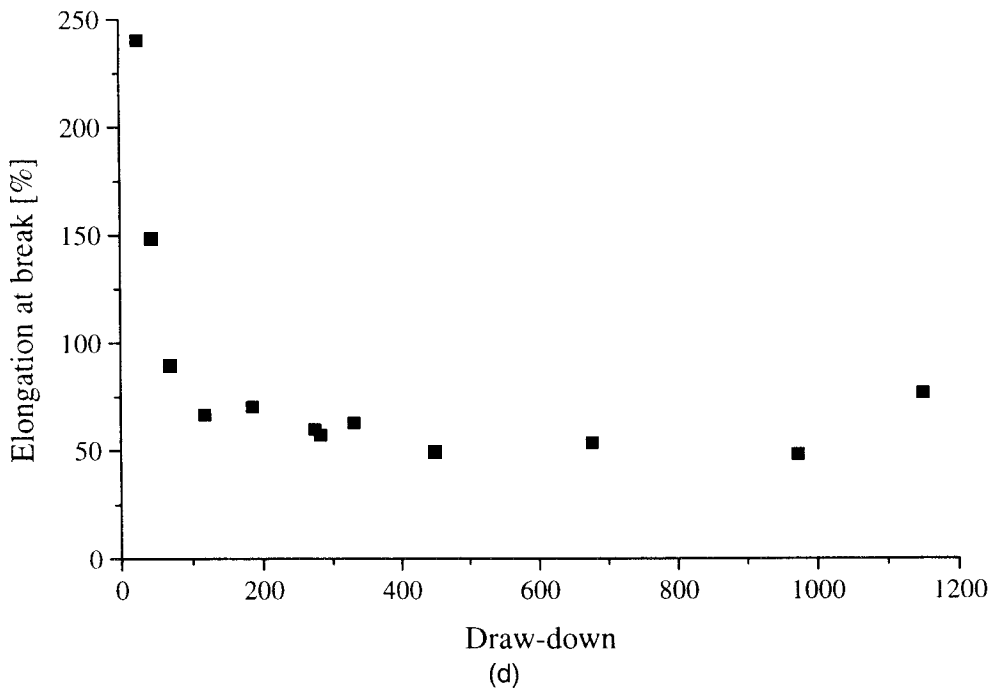
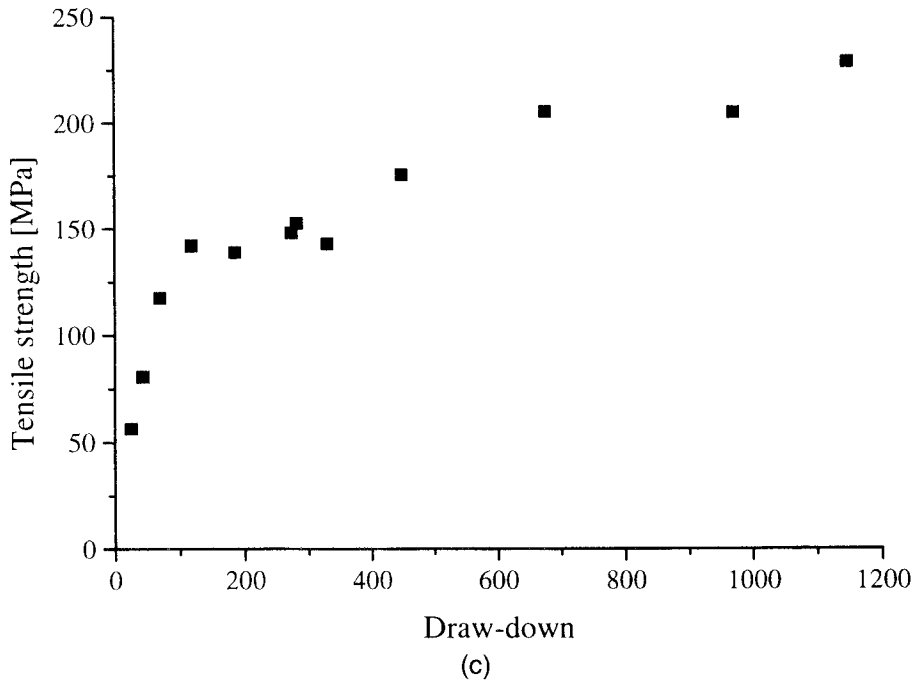


Fig. 1. Continued.

melt-spun sPP fibers is introduced. Two main different chain conformations in the crystalline state of sPP are known, a twofold helical (ttgg)₂ and the planar all-trans (ttt)_n conformation, but only cold-drawn samples exhibit a crystal structure based on the latter conformation (9–12, 19). Additional preparation routes were found to form the “all-trans” crystal phase using a special solution/melt spinning technique

and laboratory scale sPP of very high syndiotacticity (rrrr = 98%) (12). This result, together with the early studies of cold-drawn samples, yields to the assumption that stress-induced crystallization is an important factor for the formation of the all-trans phase. After all, the melt-spinning process as described in this study is an additional preparation route for the solidification of all-trans crystals.

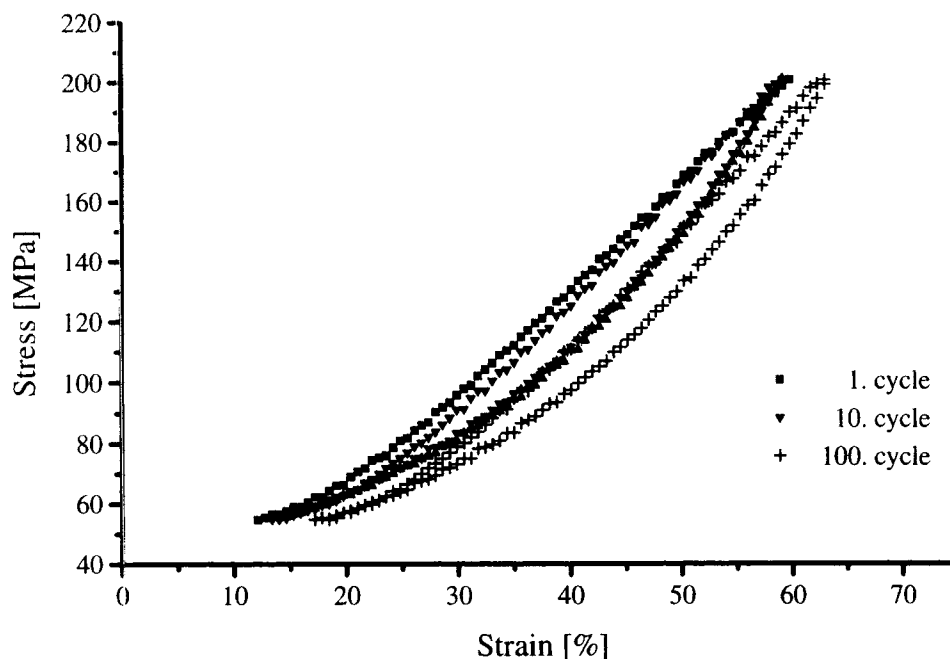
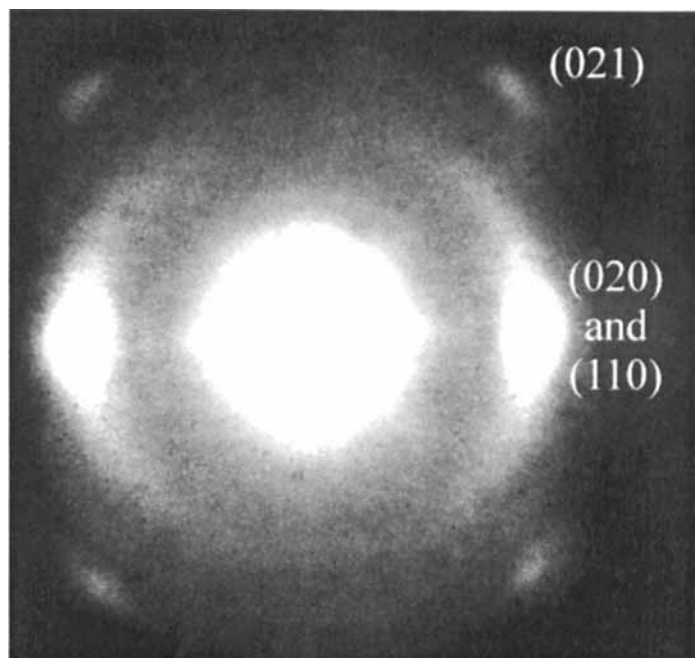


Fig. 2. Stress-strain curves of dynamic load-unload cycles for a sPP fiber with high spinning draw-down of 1150.

Fig. 3. X-ray pinhole diffraction pattern of a bundle of melt-spun sPP fibers with a high draw-down of 1150. The main diffraction reflections are indicated.



Moreover, only defect-free molecular sequences of the macromolecules longer than the critical nucleus size of the all-trans phase can contribute to its formation (12). The pre-commercial sPP used in this study has a relatively low syndiotacticity, which results in a high number of tacticity defects in the molecules. These defects, in the all-trans conformation, cause a change of the spatial direction of the chain and cannot be incorporated in the crystal. The formation of the

all-trans phase is preferred using the described preparation conditions, but the low syndiotacticity with high number of defects along the macromolecules results in low crystallinity and small micel-like crystals in the fibers. These crystals act as physical crosslinks in the amorphous matrix (Fig. 4). Finally, the morphology of the melt-spun sPP fibers is comparable with the architecture of thermoplastic elastomers. The deformation and almost complete relaxation of

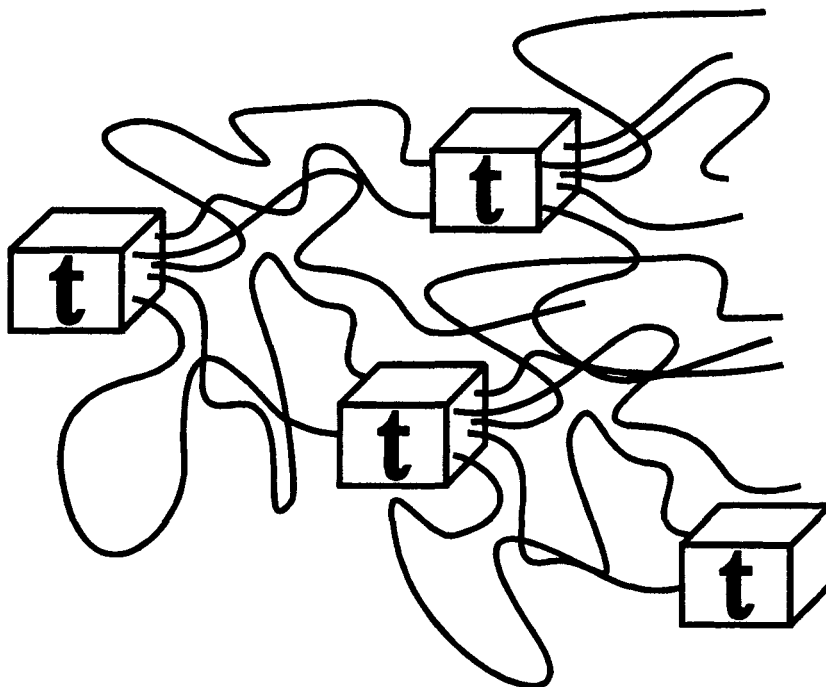


Fig. 4. Sketch of the fiber morphology: small all-trans crystals (*t*) in the amorphous matrix.

the amorphous molecule segments fixed between small crystals lead to the observed rubber-like mechanical behavior. Further investigation of the morphology and its influence on the mechanical behavior of melt-spun sPP fibers will be discussed in detail in later studies.

CONCLUSION

The melt-spinning process of sPP fibers is described. A rubber-like mechanical behavior is observed for fibers with high draw-down and determined by static and dynamic tensile tests. It is found that the fibers show almost complete elastic recovery, even after 1000 test cycles, with a upper stress limit of 80% of their average fracture stress. Released fibers show an elongation of approximately 7% after 100 cycles and 15% after 1000 cycles indicating a low plastic deformation during the dynamic test. A model is introduced explaining the rubber elastic behavior of sPP fibers with high draw-downs. The melt-spinning process favors the formation of small micel-like crystals, which are formed by molecules with planar all-trans conformation (all-trans phase), and these crystals act as physical crosslinks in the amorphous matrix.

REFERENCES

1. H. Uehara, Y. Yamazaki, C. Otake, and T. Kanamoto, *Rep. Prog. Polym. Phys. Jpn.*, **36**, 245 (1993).
2. C. DeRosa, F. Auriemma, and P. Corradini, *Macromolecules*, **29**, 7452 (1996).
3. G. Natta, P. Corradini, and P. Ganis, *Makromol. Chem.*, **39**, 238 (1960).
4. P. Corradini, G. Natta, P. Ganis, and P. Temussi, *J. Polym. Sci., Polym. Symp.*, **16**, 2477 (1967).
5. B. Lotz, A. J. Lovinger, and R. E. Cais, *Macromolecules*, **21**, 2375 (1988).
6. A. J. Lovinger, B. Lotz, and D. D. Davis, *Polymer*, **31**, 2253 (1990).
7. A. J. Lovinger, D. D. Davis, and B. Lotz, *Macromolecules*, **24**, 552 (1991).
8. C. DeRosa and P. Corradini, *Macromolecules*, **26**, 5711 (1993).
9. G. Natta, M. Peraldo, and G. Allegra, *Macromol. Chem.*, **75**, 215 (1964).
10. H. Tadokoro, M. Kobayashi, S. Kobayashi, K. Yasufuku, and K. Mori, *Rep. Prog. Polym. Phys. Jpn.*, **9**, 181 (1966).
11. Y. Chatani, H. Maruyama, K. Noguchi, T. Asanuma, and T. Shiomura, *J. Polym. Sci., Polym. Lett.*, **28**, 393 (1990).
12. J. Loos, A.-M. Schouwienold, S. Yan, J. Petermann, and W. Kaminsky, *Polym. Bull.*, **38**, 185 (1997).
13. Y. Chatani, H. Maruyama, T. Asanuma, and T. Shiomura, *J. Polym. Sci., Polym. Phys.*, **29**, 1649 (1991).
14. F. Auriemma, C. DeRosa, O. Ruiz de Ballesteros, V. Vinti, and P. Corradini, *J. Polym. Sci., Polym. Phys.*, **36**, 395 (1998).
15. S. Haftka and K. Koennecke, *J. Macromol. Sci. Phys.*, **B30**, 319 (1991).
16. H. Uehara, Y. Yamazaki, C. Otake, and T. Kanamoto, *Rep. Prog. Polym. Phys. Jpn.*, **36**, 245 (1993).
17. Y. Sakata, A. P. Unwin, and I. M. Ward, *J. Mater. Sci.*, **30**, 5841 (1995).
18. H. Uehara, Y. Yamazaki, and T. Kanamoto, *Polymer*, **37**, 57 (1996).
19. J. Loos, J. Petermann, and A. Waldoefner, *Colloid Polym. Sci.*, **275**, 1088 (1997).
20. I. Sakurada, T. Ito, and K. Nakamea, *J. Polym. Sci., Part C*, **15**, 75 (1966).
21. T. Nishino, Y. Gotoh, S. Kuroda, and K. Nakamae, private communication.
22. E. S. Shamshoum, L. Sun, B. R. Reddy, and D. Turner, "Properties and Applications of Low Density Syndiotactic Polypropylene," presented at MetCon '94, Houston, May (1994).
23. Y. Ohta and H. Yasuda, *J. Polym. Sci., Polym. Phys.*, **32**, 2241 (1994).